Eicosapentaenoic acid prevents obesity-induced metabolic impairments through the host-genetic dependent effects of resolvin E1

Anandita Pal[1*], Abrar E. Al-Shaer[1*], William Guesdon[2,], Maria J. Torres[3], Michael Armstrong[4], Kevin Quinn[4], Traci Davis[1], Nichole Reisdorph[4], P. Darrell Neufer[3], Espen E. Spangenburg[3], Ian Carroll[1], Richard P. Bazinet[5], Joan Clària[6] and Saame Raza Shaikh[1]

*both authors contributed equally

[1]Department of Nutrition, Gillings School of Public Health and School of Medicine, The University of North Carolina at Chapel Hill; [2]Department of Biochemistry & Molecular Biology, Brody School of Medicine, East Carolina University; [3]Department of Physiology, East Carolina Diabetes & Obesity Institute, East Carolina University; [4]Department of Pharmaceutical Sciences, University of Colorado Denver Anschutz Medical Campus; [5]Department of Nutritional Sciences, University of Toronto; [6]Department of Biomedical Sciences, University of Barcelona, Hospital Clínic-IDIBAPS, Barcelona, Spain.

Present address for William Guesdon: School of Immunology and Microbial Sciences, King's College London
Present address for Maria Torres: Duke Molecular Physiology Institute, Duke University

Running title: RvE1-EPA and fasting insulin/glucose

Category:
Word Count:

Corresponding author: Saame Raza Shaikh, Department of Nutrition, Gillings School of Public Health and School of Medicine, The University of North Carolina at Chapel Hill.
shaikhsa@email.unc.edu

The research was supported by: R01AT008375 (SRS), P30DK05635 (SRS), R01AR066660 (ES), NIH/NCRR S10 RR026522-01A1 (NR), R01DK096907 (PDN), Canadian Institutes of Health Research 303157 (RPB), SAF15-63674-R (Spanish Ministry of Economy and Science, JC) and 2017SGR1449 (AGAUR Generalitat de Catalunya, JC). This material is also based upon work supported by the National Science Foundation Graduate Research Fellowship Program under Grant No. 1650116 to AEA. Any opinions, findings, and conclusions or recommendations expressed in this material are those of the author(s) and do not necessarily reflect the views of the National Science Foundation. The microbiome studies were supported by the Microbiome Core Facilities, supported in part by NIDDK P30DK34987

ABSTRACT

Aims: Eicosapentaenoic acid (EPA) is consumed in low levels in the western diet. Increased consumption of EPA may prevent impairments in insulin-glucose homeostasis that contribute toward cardiometabolic disorders. Here we investigated how EPA, through the biosynthesis of its downstream metabolites, prevents metabolic impairments driven by diet-induced obesity.

Methods and Results: Long-term administration of pure EPA ethyl esters to C57BL/6J male mice improved obesity-induced glucose intolerance, hyperinsulinemia, and hyperglycemia. Supporting analyses of National Health and Nutrition Examination Survey data revealed fasting glucose levels of obese adults were inversely related to EPA intake in a sex-dependent manner and were dependent on the ratio of linoleic acid to EPA. We next investigated potential mechanisms by which EPA improved hyperinsulinemia and hyperglycemia. 16S rRNA sequencing showed EPA supplementation did not remodel the gut microbiome composition relative to obese mice. Subsequent untargeted and targeted mass spectrometry analyses revealed distinct modifications in the lipidome. Notably, EPA overturned the obesity-driven decrement in the concentration of 18-hydroxyeicosapentaenoic acid (18-HEPE) in metabolic tissues. Therefore, we probed if administration of the bioactive downstream metabolite of 18-HEPE known as resolvin E1 (RvE1) for four days could reverse hyperinsulinemia and hyperglycemia through RvE1's receptor ERV1/ChemR23. Additionally, we determined if the metabolic effects of RvE1 were dependent on host genetics. Experiments with obese ERV1/ChemR23 knockout and wild type mice showed that RvE1 mitigated hyperinsulinemia and hyperglycemia in

a manner dependent on ERV1/ChemR23. RvE1's effects on fasting insulin and glucose were not uniform in diversity outbred mice that model human genetic variation. Furthermore, secondary SNP analyses revealed extensive genetic variation in human RvE1- and EPA-metabolizing genes.

Conclusions: The data suggest increased EPA intake prevents metabolic impairments in obesity through a mechanism mediated by RvE1. The data also underscore the critical need for precision prevention studies that account for host-genetics in the EPA-RvE1 axis.

Translational Perspective: EPA ethyl esters have attracted significant attention based on findings from the REDUCE-IT trial on cardiovascular disease risk reduction. This study investigated how EPA ethyl esters prevent obesity-induced hyperinsulinemia and hyperglycemia. Our data show that EPA ethyl esters improved murine fasting insulin and glucose levels through the actions of the downstream metabolite known as resolvin E1 (RvE1). Notably, RvE1's effects on hyperinsulinemia and hyperglycemia were dependent on the host genetic profile. Collectively, these data suggest targeting the EPA-RvE1 pathway may be an effective approach for preventing impairments in insulin-glucose homeostasis in a host genetic dependent manner.

1.0 Introduction

Circulating levels of eicosapentaenoic acid (EPA, 20:5n-3) are generally low in the western population [1, 2]. Therefore, increased intake of EPA and other n-3 polyunsaturated fatty acids (PUFA) is hypothesized to ameliorate a range of risk factors that contribute toward cardiometabolic diseases [3]. Recently, EPA has garnered attention as the REDUCE-IT trial showed EPA ethyl esters substantially reduced the risk of cardiovascular disease in statin-treated patients with elevated triglycerides [4]. This has led to the FDA approval of EPA ethyl esters for cardiovascular disease risk reduction in patients with hypertriglyceridemia. EPA-containing supplements are also FDA approved for lowering elevated triglycerides, a risk factor for type 2 diabetes and cardiovascular diseases [3].

The effects of n-3 PUFAs on insulin sensitivity and glucose tolerance remain strongly debated. Several randomized clinical trials have failed to establish the benefits of increased n-3 PUFA intake for treating subjects with insulin resistance, which could be due to a range of factors including the use of inappropriate controls [3, 5, 6]. Nevertheless, the prevailing view is that n-3 PUFAs are unlikely to be an effective treatment modality for insulin-resistant individuals. In contrast, there is evidence in the preclinical literature that n-3 PUFAs may have a role in the prevention of metabolic abnormalities driven by obesity. However, a unifying mechanism by which EPA prevents insulin resistance remains unclear [3]. Furthermore, the majority of preventative studies have relied on heterogenous mixtures of n-3 PUFAs despite evidence that EPA and its long chain counterpart docosahexaenoic acid (DHA) are not structurally or functionally identical [7, 8]. Also, many preclinical studies rely on levels of n-3 PUFAs that are not

117 achievable in humans [3]. Thus, the overarching goal of this study was to address these
118 limitations.

119 We first studied if pure EPA ethyl esters, modeling human pharmacological intake,
120 prevent obesity-induced metabolic impairments using C57BL/6J mice. Supporting
121 analyses on the association between fasting glucose levels and dietary intake of PUFAs
122 was conducted using data from the National Health and Nutrition Examination Survey
123 (NHANES). Mechanistically, we first focused on the microbiome as there is evidence that
124 fish oils containing n-3 PUFAs change the composition of gut bacteria to lower systemic
125 inflammation and decrease endotoxemia, a driver of metabolic complications such as
126 insulin resistance [9-11]. Subsequently, metabolomic and lipidomic analyses were
127 conducted to identify targets of EPA ethyl esters, which led to the study of EPA-derived
128 resolvin E1 (RvE1), a specialized pro-resolving mediator (SPM) with potential
129 insulin/glucose-sensitizing properties [12-17]. We specifically investigated if exogenous
130 administration of RvE1 could reverse hyperinsulinemia and hyperglycemia through
131 RvE1's receptor ERV1/ChemR23. Furthermore, we assessed if the metabolic effects of
132 RvE1 were dependent on the host genome. To do so, we employed diversity outbred
133 (DO) mice, which are a unique mouse population that model human genetic diversity [18].
134 Additionally, we conducted SNP analyses by mining the Ensembl database to identify
135 genetic variation of EPA and RvE1 metabolizing genes in humans.
136
137
138
139

2.0 Materials and Methods

2.1 Animal models, diets, and RvE1 administration. All murine experiments adhered to IACUC guidelines established by The University of North Carolina at Chapel Hill and East Carolina University for euthanasia and humane treatment. C57BL/6J male mice of 5-6 weeks of age were fed lean control (10% kcal from lard, Envigo TD.160407) or high fat (60% kcal from lard, Envigo TD.06414) diet in the absence or presence of EPA (Cayman, ≥93%) ethyl esters (Envigo TD.160232) for 15 weeks. EPA in the high fat diet accounted for 2% of total energy. The schematic illustrating the generation of the ERV1/ChemR23 mutant allele by CRISPR/Cas9-mediated genome editing is provided in the Supplemental Materials, as described below. These mice and wild type littermate controls were also fed diets from Envigo.

For select studies, C57BL/6J male mice were purchased obese from Jackson at 18 weeks of age. They were acclimatized by feeding lean (10% lard, D12450B) or high fat (60% lard, D12492) diets (Research Diets) for an additional 2-3 weeks prior to conducting experiments. DO male mice (Jackson) from generation 33 were obtained at 4 weeks of age and acclimated for 2 weeks. The DO population is derived from 144 Collaborative Cross lines obtained from Oak Ridge National Laboratory at generations F4-F12 of inbreeding [18].

2.2 Body mass and insulin/glucose measurements. Metabolic studies including Echo-MRI experiments were conducted as previously described [19]. Briefly, mice were fasted for 5 hours prior to the establishment of baseline glucose values with a glucometer. For the

glucose tolerance test, 2.5g of dextrose (Sigma-Aldrich) per kg lean mass was administered intraperitoneally.

2.3 Studies with DO mice. Since every DO mouse is genetically unique, each mouse served as its own control. Baseline fasting insulin/glucose measurements were recorded once each DO mouse achieved ~14 grams of fat mass as measured by Echo-MRI. The mice were then allowed one week to recover and subsequently i.p. injected with 300 ng RvE1 for 4 consecutive days. Fasting glucose and fasting insulin were again measured after RvE1 administration.

2.4 Microbiome analyses. DNA from stool was isolated on King Fisher Flex automated instrument using MagMAX™ DNA protocol. Stool samples were transferred to sterile 2 ml tubes containing 200 mg of ≤106µm glass beads (Sigma) and 0.5ml of lysis/binding buffer. Qiagen TissueLyser II was used at 30Hz to carry out bead beating for 3 minutes after which samples were centrifuged at 21000 x g for 3 minutes. Subsequently, 115µl of supernatants were transferred to MME-96 deep well plates followed by addition of magnetic bead mix and isopropanol. Finally, the sample plate was placed into the King Fisher Flex instrument along with two isopropanol-based, two ethanol-based washing solution plates as well as an elution buffer plate and the MME-96 processor script was executed. Upon completion, DNA was stored in elution buffer at -20°C until further processing. 12.5 ng of total DNA was amplified using universal primers targeting the V4 region of the bacterial 16S rRNA gene1, 2. Primer sequences contained overhang

adapters appended to the 5′ end of each primer for compatibility with the Illumina sequencing platform. The complete sequences of the primers were:

515F - 5’ TCGTCGGCAGCGTCAGATGTGTATAAGAGACAGGTGCCAGCMGCCGCGGTAA 3’

806R - 5’GTCTCGTGGGCTCGGAGATGTGTATAAGAGACAGGGACTACHVGGGTWTCTAAT 3’.

Master mixes contained 12.5ng of total DNA, 0.2μM of each primer and 2x KAPA HiFi HotStart ReadyMix (KAPA Biosystems). The thermal profile for the amplification of each sample had an initial denaturing step at 95°C for 3 minutes, followed by a cycling of denaturing at 95°C for 30 seconds, annealing at 55°C for 30 seconds, a 30 second extension at 72°C (25 cycles), a 5 minutes extension at 72°C and a final hold at 4°C. Each 16S amplicon was purified using the AMPure XP reagent (Beckman Coulter). In the next step each sample was amplified using a limited cycle PCR program, adding Illumina sequencing adapters and dual-index barcodes (index 1(i7) and index 2(i5)) (Illumina) to the amplicon target. The thermal profile for the amplification had an initial denaturing step at 95°C for 3 minutes, followed by a denaturing cycle of 95°C for 30 seconds, annealing at 55°C for 30 seconds and a 30 second extension at 72°C (8 cycles), a 5 minutes extension at 72°C and a final hold at 4°C. The final libraries were again purified using the AMPure XP reagent (Beckman Coulter), quantified and normalized prior to pooling. The DNA library pool was then denatured with NaOH, diluted with hybridization buffer and heat denatured before loading on the MiSeq reagent cartridge and on the MiSeq

206 instrument. Automated cluster generation and paired–end sequencing with dual reads
207 were performed according to the manufacturer's instructions.

208 For analyses, multiplexed paired-end fastq files were produced from the
209 sequencing results of the Illumina MiSeq using the Illumina software conFig.BclToFastq.
210 The paired-end fastq files were joined into a single multiplexed, single-end fastq using the
211 software tool fastq-join. Demultiplexing and quality filtering was performed on the joined
212 results. Quality analysis reports were produced using the FastQC software.
213 Bioinformatics analysis of bacterial 16S amplicon sequencing data was conducted using
214 the Quantitative Insights Into Microbial Ecology (QIIME2) software [20]. DADA2 was used
215 for denoising, removal of chimeric sequences, and construction of amplicon sequence
216 variants (ASVs). Feature classification was preformed using the SILVA database in the
217 QIIME2 Naïve Bayes classifier (silva-132-99-nb-classifier). Shannon alpha diversity was
218 calculated using the QIIME2 q2-diversity plugin and beta diversity was calculated utilizing
219 non-metric multidimensional scaling (NMDS) with Bray-Curtis distances. All feature tables
220 generated by the QIIME2 software were imported into the Phyloseq R package and
221 normalized via DESeq2.

222

223 2.5 Untargeted mass spectrometry-based metabolomics. Adipose tissue and liver were
224 homogenized using a bead homogenizer and prepared for metabolomics using previously
225 described methods [21]. Samples were analyzed using liquid chromatography mass
226 spectrometry (LC/MS) and raw data were extracted and processed using Agilent
227 Technologies Mass Hunter Profinder Version B.08.00 (Profinder) software in combination
228 with Agilent Technologies Mass Profiler Professional Version 14 (MPP) as previously

described [21-23]. An in-house database containing METLIN, Lipid Maps, Kyoto Encyclopedia of Genes and Genomes (KEGG), and Human Metabolomics Database (HMDB) was used to annotate metabolites based on exact mass, isotope ratios, and isotopic distribution with a mass error cutoff of 10 ppm. This corresponds to annotation at Metabolomics Standards Initiative (MSI) level 3 [24].

To visualize clustering between the dietary groups we ran a principal component analysis (PCA) using all metabolites. We then determined statistically significant metabolites between obese mice and obese mice supplemented with EPA. One of the samples from the high fat diet (HF_105) was an outlier from all the other samples and was excluded from analyses. We then calculated fold changes (EPA/high fat). Next, using the validated significant metabolites with Log2 fold changes ±1.5 we standardized the abundances of the metabolites by assigning a Z-score for each sample based on the distribution of the given metabolite. We utilized the Z-scores to generate heatmaps annotated with the classification of each metabolite.

2.6 Targeted mass spectrometry-based metabololipidomics. Analyses of PUFA-derived metabolites of visceral white adipose tissue, liver, and heart was conducted as previously described [25]. Quantitation of lipid mediators was performed using two-dimensional reverse phase HPLC tandem mass spectrometry (liquid chromatography–tandem mass spectrometry). All standards and internal standards used for the LC/MS/MS analysis were purchased from Cayman Chemical (Ann Arbor, Michigan, USA). All solvents and extraction solvents were HPLC grade or better.

2.7 Analyses of NHANES database. The 2013-2014 NHANES database was mined for daily average intake of PUFAs with respect to age, sex, and BMI. We used Rv3.4.4 with the RNHANES package to retrieve the NHANES database. Graphical packages ggpubr and ggplot2 were used to generate all graphs and statistical annotations. The “Dietary Interview - Total Nutrient Intakes” section of the NHANES database was used to retrieve PUFA intake measurements based on a 24-hour dietary recall questionnaire. OGTT 2-hour glucose measurements were retrieved from the “Current Health Status” section, where BMI was retrieved from “Body Measures”. Tertiles of PUFA intake were calculated corresponding to the probability of intake at 33.3%, 67%, and 100% of the range. Normality and homogeneity of variance were tested with the Shapiro-Wilks test and Bartlett test respectively. The dataset did not satisfy the assumptions of normality and heteroscedasticity; therefore, we utilized a Kruskal-Wallis test followed by a Wilcoxon pairwise test to measure significant differences between tertiles of PUFA intake.

2.8 SNP analyses. We used the Biomart tool to mine the Ensembl Variation 98 Human Short Variants (GRCh38.p13) database for single nucleotide polymorphisms (SNPs) with minor allele frequencies at or above 5% that are contained within the 1000 genomes project or the NCBI dbSNP archive. We mined SNPs for the genes listed in the Supplemental Methods. We used the ggplot2 package in R v3.4.4 to plot all the minor allele frequencies by each allele for every gene and chromosome. White lines in the graph represent a break/gap in the minor allele frequency (MAF) distribution, for example a gene may contain MAFs ranging from 0.05-1.5 then 2.5-4.5 with a “break” between the 1.5-2.5 gap. The distances between the SNPs of different genes on the chromosomes was

274 determined using the base pair location at the last SNP of the first gene and the first SNP
275 of the second gene. Distances below 500 kilobases were considered as having a higher
276 likelihood for genetic linkage, as described by the HapMap project Haploview tool.
277 Additional details are in the Supplemental Methods.
278
279 2.9 Statistics. Data were analyzed using Graph Pad Prism Version 7.0. Statistical
280 significance relied on one-way or two-way ANOVAs followed by a post-hoc Tukey HSD
281 test if the data satisfied the assumptions of normality and homogeneity of variance tested
282 by the Shapiro-Wilks test and Bartlett test respectively. Data that failed the assumption of
283 heteroscedasticity were analyzed using a Welch ANOVA followed by a pairwise Welch T-
284 test with a Bonferroni p-value adjustment. Data sets that did not display normal
285 distributions were analyzed with a Wilcoxon pairwise test. Studies as a function of time
286 that passed the assumptions of normality and heteroscedasticity were analyzed with a
287 two-way ANOVA. For clarity, additional description of analyses for microbiome,
288 metabolomics, and NHANES datasets are included with each corresponding methods
289 section above. For all analyses, $p<0.05$ was considered statistically significant.
290
291
292
293
294
295
296

3.0 Results

3.1 EPA ethyl esters of high purity improve hyperglycemia, hyperinsulinemia, and glucose intolerance of obese male mice. We first determined if dietary administration of EPA could prevent obesity-induced metabolic outcomes of obese male mice. The approach relied on pure ethyl esters of EPA and not mixtures of EPA with DHA that can confound the data. Mice consuming a high fat diet in the absence and presence of EPA had similar increases in total mass and fat mass compared to lean controls (Fig. 1A). Inclusion of EPA in the diet of obese mice restored the obesity-driven glucose intolerance (Fig. 1B), as quantified by the area under the curve (Fig. 1C). Relative to the high fat diet, EPA restored the impairment in fasting glucose (Fig. 1D) and improved fasting insulin levels (Fig. 1E). The HOMA-IR score was lowered with EPA in the diet relative to the mice consuming the high fat diet (Fig 1F). Overall, EPA ethyl esters significantly ameliorated the metabolic insult of the high fat diet.

3.2 NHANES analyses reveal glucose levels are inversely related with EPA intake in a sex-specific manner and are also dependent on the ratio of EPA to linoleic acid. To translate the murine data, we analyzed the relation between EPA intake and blood glucose levels during an OGTT in obese humans using data from NHANES. Increased EPA intake was associated with lower glucose levels between the first and third tertiles for obese males (Fig. 2A) but not females (Fig. 2B). Furthermore, we investigated if there was a relationship between DHA and glucose levels. In obese males (Fig. 2C) and females (Fig. 2D), there was no association between DHA and blood glucose levels.

The metabolism of EPA relies on some of the same enzymes used by n-6 PUFAs such as linoleic acid (LA) [26, 27]. Thus, we further mined the NHANES data to determine if there was a relationship between the ratio of LA to EPA on fasting glucose levels. Tertiles of the LA to EPA ratio are plotted for obese men (Fig. 2E) and women (Fig. 2F). The positive association between EPA and glucose levels was diminished and in fact, at the highest ratio of LA to EPA in men (Fig. 2E), but not women (Fig. 2F), blood glucose levels were increased relative to the first two tertiles.

3.3 EPA ethyl ester supplementation does not modify the composition of the gut microbiome relative to mice on a high fat diet. Mechanistically, previous studies suggest that mixtures of EPA/DHA promote specific compositional changes in the murine microbiome in a manner that supports lower systemic inflammation associated with insulin resistance [9-11]. Therefore, we conducted a microbiome study with mice consuming control, high fat, and high fat + EPA ethyl ester diets. Using non-metric multidimensional scaling (NMDS) with Bray-Curtis distances, we found a separation in beta diversity between mice fed a control diet verses a high fat or high fat+EPA diet (Fig. 3A). However, the distances between the high fat and high fat+EPA samples were not distinctly defined, indicating small differences in the microbial beta diversity between a high fat diet and high fat+EPA diet. There were minor differences in the relative abundance between high fat and high fat+EPA diets (Fig. 3B). In contrast, the families Erysipelotrichaceae and Lactobacillaceae were decreased between mice consuming high fat diet as compared to the control diet. Shannon alpha diversity between mice fed the high fat and high fat+EPA diets were similar (Fig. 3C). The control mice had significantly

342 higher Shannon alpha diversity compared to the EPA-containing diet, suggesting a larger
343 species diversity within the control group. We found the most consistent change between
344 all three dietary groups among the proteobacteria-related microbes – spanning phylum
345 (Fig. 3D), class (gammaproteobacteria) (Fig. 3E), and order level (betaproteobacteriales)
346 (Fig. 3F). All three proteobacteria-related microbes were elevated between each dietary
347 pairwise comparison. We conducted hierarchal clustering on the samples (Fig. 3G) using
348 the normalized Log10 absolute abundance values and found that the control mice tightly
349 cluster together, whereas the high fat and high fat+EPA samples shared the same parent
350 branch in the dendrogram with little differences between their abundance values.
351 Collectively, these findings suggest that EPA ethyl esters do not improve the obesity-
352 driven compositional changes in the gut microbiome.
353
354 3.4 Metabolomic analyses reveal EPA's effects are distinct from obese mice not
355 consuming EPA. Given the mechanism of action for EPA ethyl esters is likely to be
356 pleiotropic, we conducted metabolic profiling of visceral white adipose tissue, liver, and
357 cardiac tissue from mice consuming the experimental diets. PCA plots revealed a clear
358 distinction between the control, high fat, and high fat + EPA ethyl ester diets for visceral
359 white adipose (Fig. 4A). EPA ethyl esters were predominately incorporated into
360 triglycerides with some uptake into diglycerides and phosphatidylcholine (Fig. 4B, 4C).
361 In the liver, PCA plots also showed a clear distinction between the high fat and
362 high fat + EPA ethyl ester diets (Fig. 4D). EPA ethyl esters appeared to have a broad
363 effect on the liver metabolome (Fig. 4E, 4F). EPA acyl chains were likely distributed into
364 triglycerides, phosphatidylcholine, phosphatidylethanolamine, and anandamide (Fig. 4F).

In cardiac tissue, PCA plots revealed no changes between mice consuming a high fat diet in the absence or presence of EPA (Suppl. Fig. 1). Overall, these results showed that EPA ethyl esters are incorporated into several lipid pools, which would then differentially influence metabolic pathways, particularly in the adipose tissue and liver. The full metabolite names, p-values, fold changes, and quantifications are in Supplemental Tables 1 and 2 for the adipose tissue and liver, respectively.

3.5 Targeted lipidomic analyses reveal EPA reverses the effects of obesity on the levels of 18-HEPE. We next conducted targeted metabololipidomic analyses to further study the effects of EPA on the adipose, liver, and cardiac lipidomes. The high fat diet and high fat diet + EPA modulated several n-3 and n-6 PUFA-derived metabolites in the adipose tissue (Fig. 5A) and liver (Fig. 5B). Markedly, EPA reversed the reduction of 18-HEPE levels (by up to 32-fold) in white adipose tissue (Fig. 5A) and liver (Fig. 5B) of obese mice and also increased levels relative to lean mice. EPA also strongly upregulated the concentration of 12-HEPE in white adipose tissue (Fig. 5A) and liver (Fig. 5B). In the heart, EPA had some effects on n-6 PUFA derived metabolites (Suppl. Fig. 2). The concentration of 12-HEPE and 18-HEPE were elevated by 11-27 fold relative to the lean and high fat diets in response to EPA (Suppl. Fig. 2). Overall, the strong increase of 18-HEPE in mice upon EPA intervention set the basis for subsequent experiments with RvE1, the downstream bioactive product of 18-HEPE.

3.6 Four days of administering RvE1 improves hyperinsulinemia and hyperglycemia of inbred mice in a manner that is dependent on the receptor ERV1/ChemR23. Given that

388 EPA strongly upregulated 18-HEPE, we subsequently investigated the effects of RvE1
389 on fasting insulin and glucose using C57BL/6J mice. Furthermore, we assessed if the
390 effects of RvE1 could be mediated by one of its receptors, ERV1/ChemR23. Therefore,
391 we studied the effects of short-term RvE1 treatment on ERV1/ChemR23 knockout (KO)
392 mice and wild type (WT) littermates in relation to hyperinsulinemia and hyperglycemia.
393 Supplemental Figure 3A and 3B respectively show the experimental scheme and the
394 ERV1/ChemR23 deletion allele. Body composition did not differ between obese WT and
395 ERV1/Chem23 KO mice administered vehicle control or RvE1 (Fig. 6A). RvE1
396 administered for just four days improved fasting glucose levels of WT but not
397 ERV1/ChemR23 KO mice (Fig. 6B) compared to obese mice. We also tested fasting
398 insulin levels in a subset of our WT and KO mice via an ELISA. Fasting insulin levels were
399 improved in response to RvE1 in WT obese mice but not in ERV1/ChemR23 KO obese
400 mice relative to lean animals (Fig. 6C).

401 We also determined if the effects of RvE1 on hyperglycemia and hyperinsulinemia
402 were evident in a second model system, which were C57BL/6J mice that were purchased
403 obese from Jackson Laboratories. With these mice, we did not conduct a broad lipidomic
404 analysis; however, RvE1 levels were measured via an ELISA, which showed lower levels
405 of RvE1 in the plasma of obese mice compared to lean controls (Suppl. Fig. 4). RvE1
406 administration to obese mice had no effect on body weight (Fig. 6D) compared to the
407 mice on a high fat diet. RvE1 restored fasting glucose (Fig. 6E) and improved fasting
408 insulin levels relative to obese mice (Fig. 6F).
409

3.7 Host genetics have a role in regulating the response to RvE1. Humans are genetically heterogenous; therefore, we determined whether host genetic differences lead to variations in the fasting insulin and fasting glucose response to RvE1. For these studies, we relied on DO mice that model human genetic variability [18]. Administration of a high fat diet led to large variations in body weight with DO mice. Thus, we optimized an experimental design (Fig. 7A) to measure the effects of RvE1 on fasting insulin and fasting glucose. We administered RvE1 to those mice that achieved ~14g of fat mass (measured via Echo-MRI) over the course of the period of dietary intervention with a high fat diet. The rationale for selecting ~14g of fat mass was based on the studies with obese C57BL/6J mice (Figs. 1, 6) that were in this range of fat mass. Body weight gain of the DO mice is depicted in Suppl. Fig. 5. Relative to baseline, RvE1 improved fasting glucose (Fig. 7B) and fasting insulin (Fig. 7C) levels in approximately half of the obese DO mice. In contrast, using the same experimental design with C57BL/6J mice, fasting glucose (Fig. 7D) and fasting insulin (Fig. 7E) were more uniformly improved in response to RvE1.

Data with the DO mice led us to investigate if there is strong genetic variation in RvE1- and EPA-metabolizing genes in humans. We mined the Ensembl database containing the dbSNP archive and 1000 genomes data (Suppl. Table 3). We extracted all the CYP450 enzymes that have the capacity to metabolize EPA, further downstream enzymes leading to the production of E-series resolvins (COX2, ALOX5, FLAP, ALOX12/15, LTA4H), and the two RvE1 receptors (ChemR23 and BLT1) [28-30]. The analyses show a large range of minor allele frequencies where SNPs for each gene are contained in chromosomes 1, 10, 12-15, 17 and 19 with BLT1 lacking SNPs in chromosome 14 (Fig. 7F). Genes with lower ranges of minor allele frequencies (MAF)

ranging from 0.05 (5%) – 0.38 (38%) include BLT1, COX2, CYP2J2, CYP1A1 and CYP1A2. Surprisingly, all other genes contained many high MAFs with numerous SNPs in the 0.4 (40%) - 0.5 (50%) range (Fig. 7F). Moreover, the CYP450 genes contained many SNPs in close proximity (<500 kilobases) on the same chromosome, these include: CYP2C18 and CYP2C19 (~27 Kb apart), CYP2C19 and CYP2C9 (~84 Kb), CYP2C9 and CYP2C8 (~47 Kb), CYPA1A1 and CYPA1A2 (~24 Kb), CYP4F8 and CYP4F3 (~10 Kb), CYP4F3 & CYP4F12 (~10 Kb), and CYP4F12 and CYP4F2 (~181 Kb). Taken together, these results showed high population variance in EPA- and RvE1- metabolizing genes.

4.0 Discussion

There is growing evidence from humans and rodents that obesity impairs the biosynthesis of SPMs and their precursors, which are predominately generated from dietary n-3 PUFAs including EPA [14, 19, 31, 32]. The loss of SPMs contributes toward a range of cardiometabolic complications including chronic inflammation, hepatic steatosis, insulin resistance, susceptibility to infection, and delayed wound healing [13, 15, 25, 32-35]. Therefore, there is a critical need to understand how specific dietary n-3 PUFAs through the biosynthesis of their downstream metabolites regulate outcomes in cardiometabolic diseases. This study reveals that administration of EPA ethyl esters can prevent hyperinsulinemia and hyperglycemia through the actions of RvE1 in a host genetic dependent manner.

The analyses of the NHANES data underscore the need for preventative precision nutrition studies with EPA. Longitudinal studies with EPA that are focused on prevention, prior to the onset of insulin resistance, are lacking. One pilot study demonstrated that administration of n-3 PUFAs to healthy human volunteers prevented insulin resistance induced with a glucocorticoid [36]. Our NHANES analyses revealed those subjects with lowest consumption of EPA, but not DHA, had the highest glucose levels in a sex-specific manner. The positive effects of EPA were mitigated when the intake of LA was high. While these data are associative, they point to the importance of discriminating EPA from DHA and accounting for LA levels in clinical studies and trials. LA is of significance for several reasons. LA biosynthesis and metabolism requires some of the same enzymes used for EPA synthesis and metabolism, including the production of downstream metabolites such as RvE1 [26, 27]. Moreover, LA's consumption in the western diet is 14-

479 18 times the amount required to prevent LA deficiency [2, 37] and LA's effects on insulin
480 sensitivity are strongly debated [38].

481 The data with EPA ethyl esters challenge some previous findings. Earlier studies
482 reported a reduction in fat mass with EPA-enriched oils, which we did not observe [39,
483 40]. Additionally, EPA did not promote changes in the composition of the gut microbiota
484 induced by a high fat diet. Some studies show that fish oils or fat-1 transgenic mice
485 remodel the gut microbiome to lower the abundance of Gram negative bacteria [9-11].
486 EPA ethyl esters are clearly remodeling several lipid pools, which may in turn influence
487 metabolites generated by the gut microbiome. Therefore, it is possible that EPA ethyl
488 esters are promoting changes in microbial metabolites. Nevertheless, our data with EPA
489 ethyl esters do not match previous findings on body weight or the microbiome, which we
490 speculate is driven by the concentration, duration, and use of EPA/DHA mixtures. EPA
491 driving an upregulation in the concentration of RvE1's precursor is highly consistent with
492 a recent clinical trial to show that consumption of an n-3 PUFA supplement promoted a
493 strong upregulation of SPMs within 24 hours [41].

494 RvE1 is likely exerting its effects through multiple mechanisms. We discovered that
495 four days of administering RvE1 rescued hyperglycemia and hyperinsulinemia through
496 ERV1/ChemR23. There is evidence that RvE1 blocks signaling through BLT1, the
497 receptor for the arachidonic acid-derived LTB4 [16]. LTB4 serves as a chemokine for
498 select immune cell populations that exacerbate glucose intolerance [42]. Thus, RvE1 may
499 also be inhibiting LTB4 binding to BLT1 to improve chronic inflammation. RvE1 may also
500 be inhibiting signaling through chemerin, an adipokine that binds ERV1/ChemR23 [43].
501 At the organ and cellular level, RvE1 can improve inflammation though the targeting of

intestinal alkaline phosphatase and specific cell types including neutrophils [35, 44, 45]. An additional possibility is that RvE1 may exert its effects through the production of further downstream metabolites. This may explain why we did not detect RvE1 as the SPM may be undergoing increased turnover to oxidized metabolites [32]. Our mass spectrometry assay did not include downstream metabolites like 18-oxo-RvE1. In addition, it is possible that administering other metabolites such as RvE2 or 12-HEPE could further improve outcomes. We did not study the effect of 12-HEPE, which is of interest as it was recently identified to improve glucose metabolism [46].

There is some ambiguity among studies regarding the effects of RvE1 on hyperglycemia. Overexpression of ERV1/ChemR23 in myeloid cells improved hyperglycemia and hepatic steatosis of male mice [47]. However, RvE1 administration to wild type mice at a dose of 2ng/g body weight twice weekly for four weeks did not improve hyperglycemia [47]. Our studies relied on a dose of RvE1 (300ng/mouse) for four consecutive days, which may explain the positive effects. Overall, our data on RvE1 were in agreement with the literature to show that select DHA-derived SPMs improve insulin resistance [13, 17, 33, 48, 49]. For instance, the DHA-derived SPM protectin D1 alleviates insulin resistance by controlling skeletal muscle IL-6 secretion and resolvin D1 enhances glucose tolerance by targeting adipose tissue inflammation [13, 17].

An additional advancement from this study is that DO mice, which model human genetic diversity, respond in a divergent manner upon RvE1 administration. The results break new ground by suggesting that RvE1 is unlikely to have a uniform positive effect in all obese humans. Overall, little is known about the role of host genetics on SPM biology. One study highlights the importance of genetic variation by demonstrating that obese

525 subjects with a C allele in the rs1878022 polymorphism of ERV1/ChemR23 receptor
526 confers protection from adipose tissue inflammation [50]. Mining the 1000 genomes and
527 dbSNP databases revealed a large range of minor allele frequencies in the EPA and
528 RvE1-metabolizing genes. Most of the genes analyzed reach minor allele frequencies
529 close to 50%, indicating large population variance in the EPA-RvE1 pathway.
530 Furthermore, close proximity of the CYP450 enzyme SNPs suggest potential genetic
531 linkage in many of the CYP450 variants that can potentially influence metabolism of EPA
532 and its downstream metabolites. The results provide strong groundwork for future
533 genetics studies that will establish candidate genes regulating the metabolic response to
534 RvE1. This will allow investigators to establish ‘responders’ from ‘non-responders’ to
535 SPMs in humans. Overall, these data highlight the need for precision administration of
536 EPA and RvE1 based on host genetic profiles.

537 In summary, the results provide strong evidence that the EPA-RvE1 axis has a
538 critical role in controlling insulin and glucose homeostasis, which may be a preventative
539 target for cardiometabolic diseases. The results across model systems highlight the need
540 for future prevention studies that account for the role of host genetics in the metabolism
541 of RvE1 and other EPA-derived metabolites.

542

543

544

545

546

547

548 **Figure Legends**

549

550 **Figure 1. EPA ethyl esters prevent obesity-induced impairments in glucose**
551 **tolerance, fasting glucose and fasting insulin levels of C57BL/6J mice.** (A) Body
552 composition measured by Echo-MRI. (B) Glucose tolerance test performed by intraperitoneal
553 injection of glucose after a 5 hour fast. (C) Area under the curve (AUC), calculated by
554 integration of the curves in B normalized to baseline values. (D) Fasting glucose and (E)
555 fasting insulin levels after a 5 hour fast. (F) HOMA-IR scores. For all measurements, male
556 mice consumed a lean control (Con) diet (O), a high fat (HF) diet (Δ), or a HF diet
557 supplemented with EPA ethyl esters (□). Measurements were conducted at week 13 of
558 intervention. Values are means ± SD. *p<0.05, **p<0.01, ***p<0.001, ****p<0.0001 from one-
559 way ANOVA followed by Tukey's multiple comparisons test except B, which was a two-way
560 ANOVA followed by a post hoc test.

561

562 **Figure 2. Glucose levels are inversely related to EPA intake in obese men but not**
563 **women and are dependent on the ratio of LA to EPA.** NHANES data on two-hour
564 glucose measurements (mg/dl) from an OGTT were stratified by tertiles of EPA intake in
565 grams for obese (A) males and (B) females. DHA intake is also depicted for (C) males
566 and (D) females. The range of EPA intake for males was 0.0-0.009g for tertile 1, 0.01-
567 0.068g for tertile 2, 0.069g and above for tertile 3. For females, the intake is 0-0.009 for
568 tertile 1, 0.01-1.51g for tertile 2, 1.52g and above for tertile 3. The range of DHA intake
569 for males is 0.01-0.05g for tertile 1, 0.06-1.49g for tertile 2, and 1.5g and above for tertile
570 3. The range of DHA intake for females was 0.01-0.03g for tertile 1, 0.04-2.35g for tertile

571 2, and 2.36g and above for tertile 3. Subjects were adults (18 years and older) and had a
572 BMI of 30 and above. Tertiles of the ratio of LA to EPA are presented for obese (E) males
573 and (F) females. The tertiles correspond to 33%, 67%, and 100% of the range of LA to
574 EPA intake for subjects older than 18 and a BMI of 30 and above. Values are means ±
575 SEM; *p<0.05, **p<0.01, ***p<0.001. from Wilcoxon pairwise test. Number of subjects for
576 each tertile is listed on the x-axis.
577
578 **Figure 3. EPA ethyl esters do not improve obesity-driven modifications to the gut**
579 **microbiome.** C57BL/6J male mice consumed either a control (Con), high fat (HF) or
580 HF+EPA ethyl ester diet. (A) NMDS plot with Bray-Curtis distances portraying beta-
581 diversity between samples. (B) Family level relative abundances calculated from
582 normalized absolute abundances. (C) Shannon alpha diversity between diet groups
583 calculated by QIIME2. (D) Log10 normalized absolute abundance of phylum level
584 proteobacteria. (E) Log10 normalized absolute abundance of class level
585 gammaproteobacteria. (F) Log10 normalized absolute abundance of order level
586 betaproteobacteriales. (G) Heatmap of Log10 normalized absolute abundances with
587 hierarchal complete linkage clustering of the taxa (columns) and samples (rows). Fecal
588 samples were collected at week 13 of intervention. Values are means ± SD; *p<0.05,
589 **p<0.01, ***p<0.001 from Wilcoxon pairwise test. n=8-11 mice per diet.
590
591 **Figure 4. EPA ethyl esters have a distinct metabolic profile in white adipose tissue**
592 **and liver of obese C57BL/6J male mice.** C57BL/6J male mice consumed a control
593 (Con), high fat (HF) and HF+EPA ethyl ester diet. (A) PCA plot of validated adipose tissue

metabolites between control, HF, and HF+EPA samples. (B) Heatmap of Z-scores from significant adipose tissue metabolites with ±1.5 fold-change. (C) Log2 fold change graph of EPA-containing (20:5) adipose metabolites. (D) PCA plot of validated liver metabolites between control, HF, and HF+EPA samples. (E) Heatmap of Z-scores from significant liver metabolites with ±1.5 fold-change. (F) Log2 fold change graph of EPA-containing (20:5) adipose metabolites. Heatmap legends on the right hand side of (B) and (E) show each metabolite's classifications: triglyceride (TG), diacylglycerol (DG), phosphatidylethanolamine (PE), lysophosphatidylethanolamine (LysoPE), phosphatidic acid (PA), phosphatidylcholine (PC), phosphatidylserine (PS), phosphatidylglycerol (PG), phosphatidylinositol (PI), arachidonoylethanolamine (AEA), cholesterol (CL), and docosahexaenoic acid (DHA). Full metabolite names are provided in the supplemental.

Figure 5. EPA ethyl esters reverse the effects of obesity on 18-HEPE of C57BL/6J mice. Mass spectrometry based metabololipidomic analyses of (A) visceral white adipose tissue and (B) liver. Metabolites from eicosapentaenoic acid (EPA), docosahexaenoic acid (DHA), linoleic acid (LA) and arachidonic acid (AA) are depicted in the heat map. Male mice consumed experimental diets for 15 weeks. N=4-5 mice per diet. Data are average. *p<0.05, **p<0.01, ***p<0.001 as compared to a control diet and $^{+}$p<0.05, $^{++}$p<0.01 as compared to the high fat diet. Statistical analyses for these data are described in the methods section.

Figure 6. Four days of administering RvE1 to C57BL/6J mice improves obesity-driven impairments in fasting glucose and insulin, mediated by the receptor

ERV1/ChemR23. (A) Body weight (B) fasting glucose and (C) fasting insulin levels of male wild type (WT) and ERV1/ChemR23 knockout (KO) mice consuming a lean control diet (Con) (O) or high fat (HF) diet in the absence (Δ) or presence (□) of RvE1. Corresponding (D) body weight, (E) fasting glucose and (F) fasting insulin levels of C57BL/6J male mice purchased as obese from Jackson Laboratories. All measurements were made at 13-14 weeks of dietary intervention. N=14-18 mice per diet (A,B), N=6-7 mice per diet (C), N=14 mice per diet (D-F). Values are means ± SD. *p<0.05, **p<0.01, ***p<0.001, ****p<0.0001 by one-way ANOVA followed by Tukey's multiple comparisons test.

Figure 7. Host genetics have a critical role in the metabolic response to RvE1. (A) Schematic representation of study design with diversity outbred mice. Fasting glucose and insulin measurements were obtained prior to (baseline) and after 4 days of RvE1 administration. (B) Fasting glucose and (C) fasting insulin levels after a 5 hour fast. Corresponding studies with C57BL/6J mice using the same experimental design of intervention are depicted for (D) fasting glucose and (E) fasting insulin. All data are plotted as the fold change in glucose and insulin relative to baseline. N =19 DO mice and N= 6 C57BL/6J mice. **p<0.01 by a paired two-tailed t test. (F) Data were mined from the 1000 genomes and dbSNP human variants databases. Snalyses show SNPs in the EPA and RvE1 metabolizing genes stratified by each minor allele (A,C,G,T). The SNPs in each gene are plotted by minor allele frequencies and the chromosome that contains the SNP. The major genes that metabolize EPA and/or RvE1 are depicted by differing colors.

Author contributions. A.P. designed and conducted experiments, wrote the manuscript, analyzed data; A.E.A. designed and conducted experiments, wrote parts of the

639 manuscript, analyzed data; W.G. designed and conducted experiments, analyzed data;
640 M.T. conducted experiments; M.A. conducted experiments and analyzed data; K.Q.
641 conducted experiments and analyzed data; T.D. conducted experiments; N.R. designed
642 experiments and provided intellectual input on select analyses; P.D.N. designed
643 experiments; E.E.S. conducted and designed experiments and provided intellectual input
644 on select experiments; I.C. designed experiments and analyzed data; R.B. designed
645 experiments and analyzed data; J. C. provided intellectual input on select data sets and
646 contributed toward editing, and S.R.S. designed experiments, analyzed data, wrote parts
647 of the manuscript and directed the overall research.
648
649 **Acknowledgements.** We thank Dr. Dale Cowley from the UNC Animal Models Core for
650 his assistance in generating the ERV1/ChemR23 KO mice and UNC's Microbiome Core
651 Facilities.
652
653 **Conflict of Interest**: RPB has received industrial grants, including those matched by the
654 Canadian government, and/or travel support related to work on brain fatty acid uptake
655 from Arctic Nutrition, Bunge Ltd., DSM, Fonterra, Mead Johnson, Nestec Inc., and
656 Pharmavite. Moreover, RPB is on the executive of the International Society for the Study
657 of Fatty Acids and Lipids and held a meeting on behalf of Fatty Acids and Cell Signaling,
658 both of which rely on corporate sponsorship. RPB has given expert testimony in relation
659 to supplements and the brain. SRS has previously received industry grants including
660 research related to n-3 fatty acids from GSK and Organic Technologies.

References

1. Stark, K.D., et al., *Global survey of the omega-3 fatty acids, docosahexaenoic acid and eicosapentaenoic acid in the blood stream of healthy adults.* Prog Lipid Res, 2016. **63**: p. 132-52.
2. Blasbalg, T.L., et al., *Changes in consumption of omega-3 and omega-6 fatty acids in the United States during the 20th century.* The American Journal of Clinical Nutrition, 2011. **93**(5): p. 950-962.
3. Lalia, A.Z. and I.R. Lanza, *Insulin-Sensitizing Effects of Omega-3 Fatty Acids: Lost in Translation?* Nutrients, 2016. **8**(6).
4. Bhatt, D.L., et al., *Cardiovascular Risk Reduction with Icosapent Ethyl for Hypertriglyceridemia.* N Engl J Med, 2019. **380**(1): p. 11-22.
5. Brown, T.J., et al., *Omega-3, omega-6, and total dietary polyunsaturated fat for prevention and treatment of type 2 diabetes mellitus: systematic review and meta-analysis of randomised controlled trials.* BMJ, 2019. **366**: p. l4697.
6. Telle-Hansen, V.H., L. Gaundal, and M.C.W. Myhrstad, *Polyunsaturated Fatty Acids and Glycemic Control in Type 2 Diabetes.* Nutrients, 2019. **11**(5).
7. Leng, X., et al., *All n-3 PUFA are not the same: MD simulations reveal differences in membrane organization for EPA, DHA and DPA.* Biochimica et Biophysica Acta (BBA) - Biomembranes, 2018.**1860:** p.1125-1134.
8. Klingel, S.L., et al., *EPA and DHA have divergent effects on serum triglycerides and lipogenesis, but similar effects on lipoprotein lipase activity: a randomized controlled trial.* Am J Clin Nutr, 2019. **110**: p.1502-1509.
9. Kaliannan, K., et al., *A host-microbiome interaction mediates the opposing effects of omega-6 and omega-3 fatty acids on metabolic endotoxemia.* Sci Rep, 2015. **5**: p. 11276.
10. Caesar, R., et al., *Crosstalk between Gut Microbiota and Dietary Lipids Aggravates WAT Inflammation through TLR Signaling.* Cell Metab, 2015. **22**(4): p. 658-68.
11. Bidu, C., et al., *The Transplantation of omega3 PUFA-Altered Gut Microbiota of fat-1 Mice to Wild-Type Littermates Prevents Obesity and Associated Metabolic Disorders.* Diabetes, 2018. **67**(8): p. 1512-1523.
12. Arita, M., et al., *Stereochemical assignment, antiinflammatory properties, and receptor for the omega-3 lipid mediator resolvin E1.* J Exp Med, 2005. **201**(5): p. 713-22.
13. Hellmann, J., et al., *Resolvin D1 decreases adipose tissue macrophage accumulation and improves insulin sensitivity in obese-diabetic mice.* FASEB J, 2011. **25**(7): p. 2399-407.
14. Neuhofer, A., et al., *Impaired Local Production of Proresolving Lipid Mediators in Obesity and 17-HDHA as a Potential Treatment for Obesity-Associated Inflammation.* Diabetes, 2013. **62**(6): p. 1945-1956.
15. González-Périz, A., et al., *Obesity-induced insulin resistance and hepatic steatosis are alleviated by ω-3 fatty acids: a role for resolvins and protectins.* The FASEB Journal, 2009. **23**(6): p. 1946-1957.
16. Sima, C., B. Paster, and T.E. Van Dyke, *Function of Pro-Resolving Lipid Mediator Resolvin E1 in Type 2 Diabetes.* Crit Rev Immunol, 2018. **38**(5): p. 343-365.

17. White, P.J., et al., *Protectin DX alleviates insulin resistance by activating a myokine-liver glucoregulatory axis.* Nat Med, 2014. **20**(6): p. 664-9.
18. Churchill, G.A., et al., *The Diversity Outbred mouse population.* Mamm Genome, 2012. **23**(9-10): p. 713-8.
19. Crouch, M.J., et al., *Frontline Science: A reduction in DHA-derived mediators in male obesity contributes toward defects in select B cell subsets and circulating antibody.* J Leukoc Biol, 2019. **106**:241-257.
20. Bolyen, E., et al., *Reproducible, interactive, scalable and extensible microbiome data science using QIIME 2.* Nat Biotechnol, 2019. **37**(8): p. 852-857.
21. Yang, Y., et al., *New sample preparation approach for mass spectrometry-based profiling of plasma results in improved coverage of metabolome.* Journal of Chromatography A, 2013. **1300**: p. 217-226.
22. Cruickshank-Quinn, C.I., et al., *Transient and persistent metabolomic changes in plasma following chronic cigarette smoke exposure in a mouse model.* PLoS One, 2014. **9**(7): p. e101855.
23. Quinn, K.D., et al., *Dysregulation of metabolic pathways in a mouse model of allergic asthma.* Allergy, 2017. **72**(9): p. 1327-1337.
24. Sumner, L.W., et al., *Proposed minimum reporting standards for chemical analysis Chemical Analysis Working Group (CAWG) Metabolomics Standards Initiative (MSI).* Metabolomics, 2007. **3**(3): p. 211-221.
25. Kosaraju, R., et al., *B Cell Activity Is Impaired in Human and Mouse Obesity and Is Responsive to an Essential Fatty Acid upon Murine Influenza Infection.* The Journal of Immunology, 2017.**198:** p.4738-4752.7.
26. Choque, B., et al., *Linoleic acid: between doubts and certainties.* Biochimie, 2014. **96**: p. 14-21.
27. Innes, J.K. and P.C. Calder, *Omega-6 fatty acids and inflammation.* Prostaglandins, Leukotrienes and Essential Fatty Acids, 2018. **132**: p. 41-48.
28. Westphal, C., A. Konkel, and W.H. Schunck, *CYP-eicosanoids--a new link between omega-3 fatty acids and cardiac disease?* Prostaglandins Other Lipid Mediat, 2011. **96**(1-4): p. 99-108.
29. Fer, M., et al., *Metabolism of eicosapentaenoic and docosahexaenoic acids by recombinant human cytochromes P450.* Arch Biochem Biophys, 2008. **471**(2): p. 116-25.
30. Fromel, T., et al., *Cytochrome P4502S1: a novel monocyte/macrophage fatty acid epoxygenase in human atherosclerotic plaques.* Basic Res Cardiol, 2013. **108**(1): p. 319.
31. Lopez-Vicario, C., et al., *Leukocytes from obese individuals exhibit an impaired SPM signature.* FASEB J, 2019. **33:** p.7072-7083
32. Clària, J., et al., *Resolvin D1 and Resolvin D2 Govern Local Inflammatory Tone in Obese Fat.* The Journal of Immunology, 2012. **189**(5): p. 2597-2605.
33. Titos, E., et al., *Signaling and Immunoresolving Actions of Resolvin D1 in Inflamed Human Visceral Adipose Tissue.* J Immunol, 2016. **197**(8): p. 3360-3370.
34. Tang, Y., et al., *Proresolution therapy for the treatment of delayed healing of diabetic wounds.* Diabetes, 2013. **62**(2): p. 618-27.
35. Freire, M.O., et al., *Neutrophil Resolvin E1 Receptor Expression and Function in Type 2 Diabetes.* J Immunol, 2017. **198**(2): p. 718-728.

36. Delarue, J., et al., *Interaction of fish oil and a glucocorticoid on metabolic responses to an oral glucose load in healthy human subjects.* Br J Nutr, 2006. **95**(2): p. 267-72.
37. Naughton, S.S., et al., *Linoleic acid and the pathogenesis of obesity.* Prostaglandins Other Lipid Mediat, 2016. **125**: p. 90-9.
38. Jandacek, R.J., *Linoleic Acid: A Nutritional Quandary.* Healthcare (Basel), 2017. **5**(2).
39. Pinel, A., et al., *EPA prevents fat mass expansion and metabolic disturbances in mice fed with a Western diet.* Journal of Lipid Research, 2016. **57**: p.1382-1397.
40. Pahlavani, M., et al., *Eicosapentaenoic acid regulates brown adipose tissue metabolism in high-fat-fed mice and in clonal brown adipocytes.* The Journal of Nutritional Biochemistry, 2017. **39**: p. 101-109.
41. Souza, P.R., et al., *Enriched Marine Oil Supplements Increase Peripheral Blood Specialized Pro-Resolving Mediators Concentrations and Reprogram Host Immune Responses: A Randomized Double-Blind Placebo-Controlled Study.* Circ Res, 2020. **126**(1): p. 75-90.
42. Li, P., et al., *LTB4 promotes insulin resistance in obese mice by acting on macrophages, hepatocytes and myocytes.* Nat Med, 2015. **21**(3): p. 239-247.
43. Mariani, F. and L. Roncucci, *Chemerin/chemR23 axis in inflammation onset and resolution.* Inflammation Research, 2015. **64**(2): p. 85-95.
44. Campbell, E.L., et al., *Resolvin E1-induced intestinal alkaline phosphatase promotes resolution of inflammation through LPS detoxification.* Proc Natl Acad Sci U S A, 2010. **107**(32): p. 14298-303.
45. Herrera, B.S., et al., *Impact of resolvin E1 on murine neutrophil phagocytosis in type 2 diabetes.* Infect Immun, 2015. **83**(2): p. 792-801.
46. Leiria, L.O., et al., *12-Lipoxygenase Regulates Cold Adaptation and Glucose Metabolism by Producing the Omega-3 Lipid 12-HEPE from Brown Fat.* Cell Metab, 2019. **30**(4): p. 768-783 e7.
47. Sima, C., et al., *ERV1 Overexpression in Myeloid Cells Protects against High Fat Diet Induced Obesity and Glucose Intolerance.* Sci Rep, 2017. **7**(1): p. 12848.
48. Jung, T.W., et al., *Protectin DX ameliorates palmitate-induced hepatic insulin resistance through AMPK/SIRT1-mediated modulation of fetuin-A and SeP expression.* Clin Exp Pharmacol Physiol, 2019. **46**: p.898-909.
49. White, P.J., et al., *Transgenic Restoration of Long-Chain n-3 Fatty Acids in Insulin Target Tissues Improves Resolution Capacity and Alleviates Obesity-Linked Inflammation and Insulin Resistance in High-Fat–Fed Mice.* Diabetes, 2010. **59**(12): p. 3066-3073.
50. Lopez-Vicario, C., et al., *Association of a variant in the gene encoding for ERV1/ChemR23 with reduced inflammation in visceral adipose tissue from morbidly obese individuals.* Sci Rep, 2017. **7**(1): p. 15724.

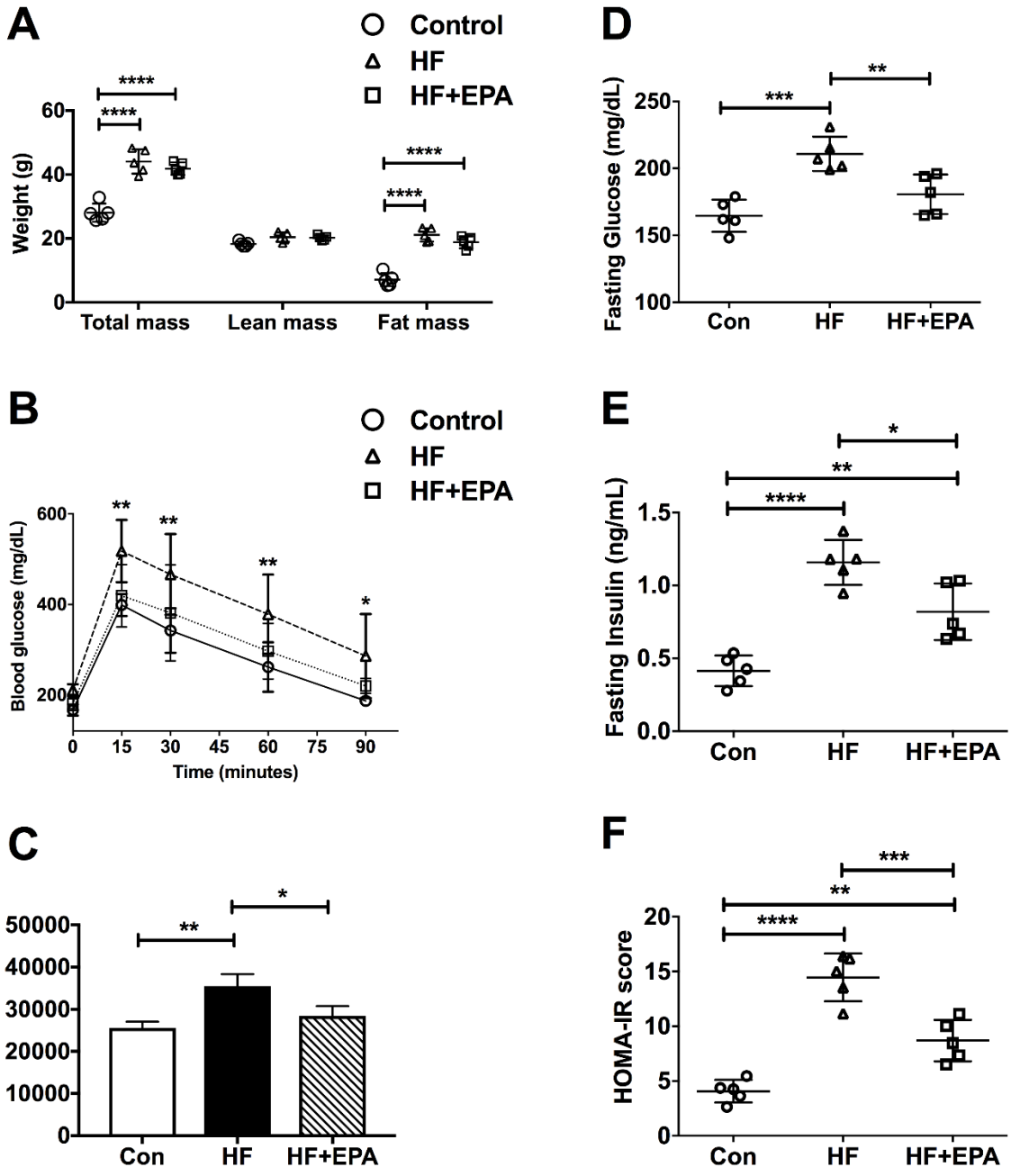

Figure 1.

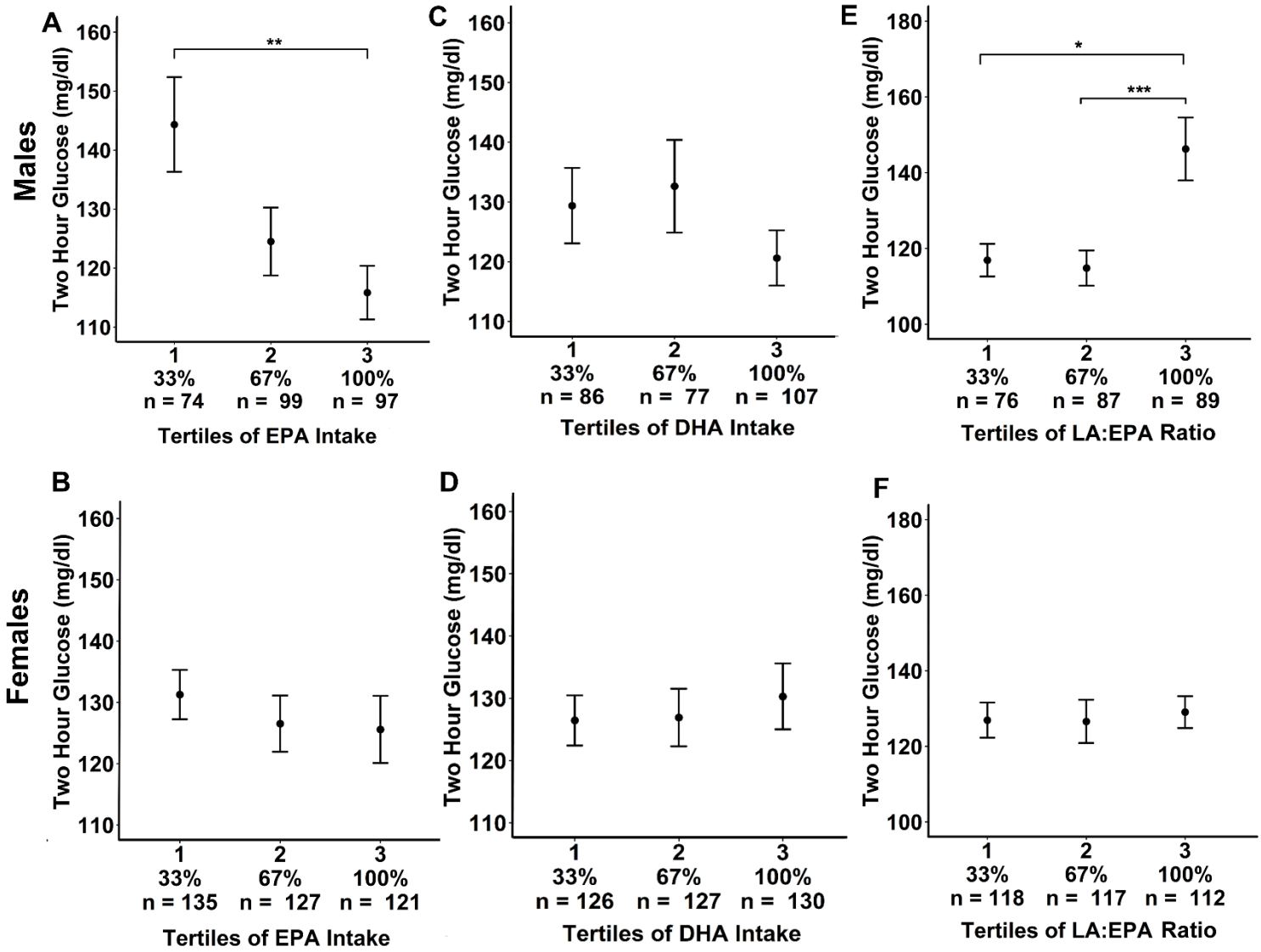

Figure 2.

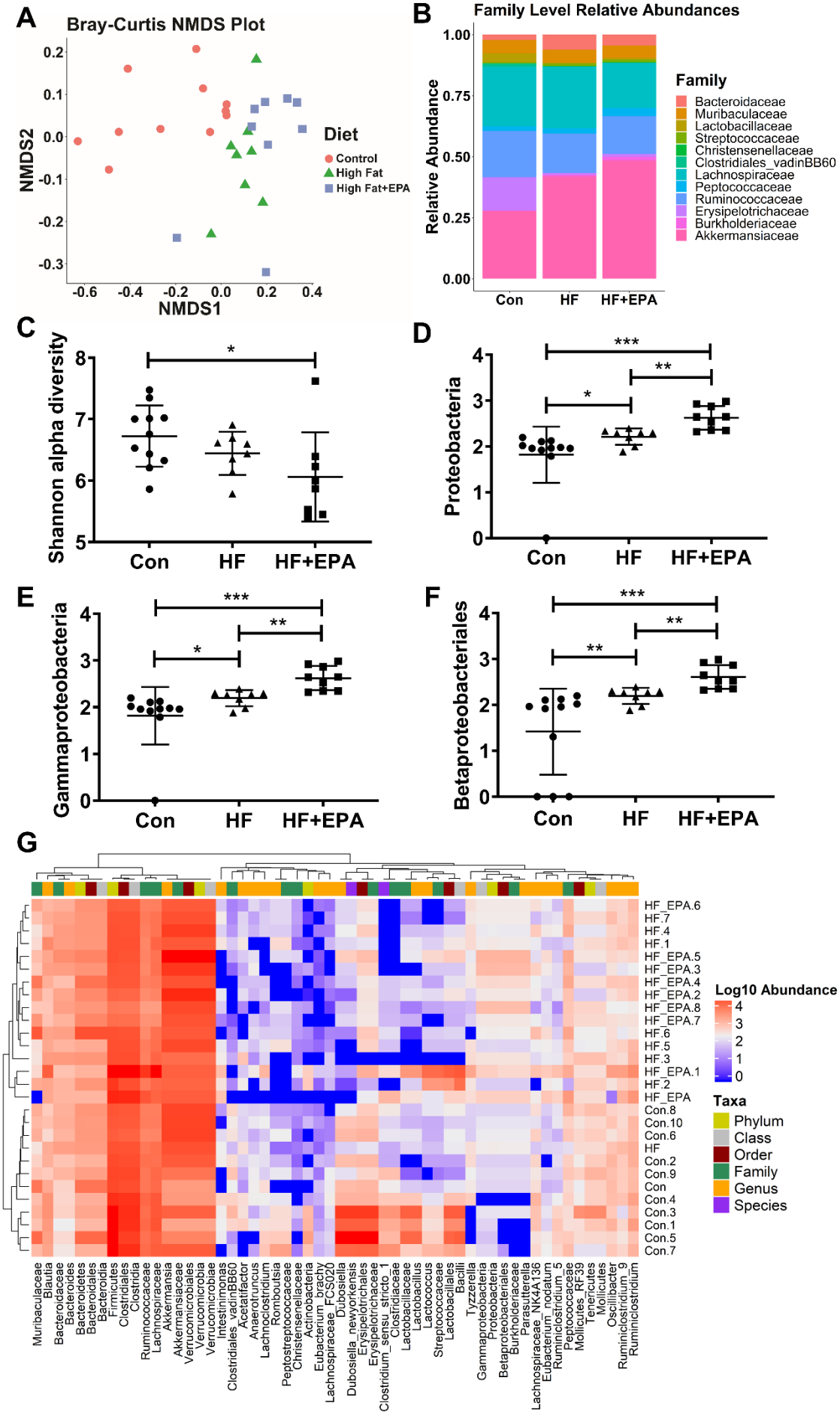

Figure 3.

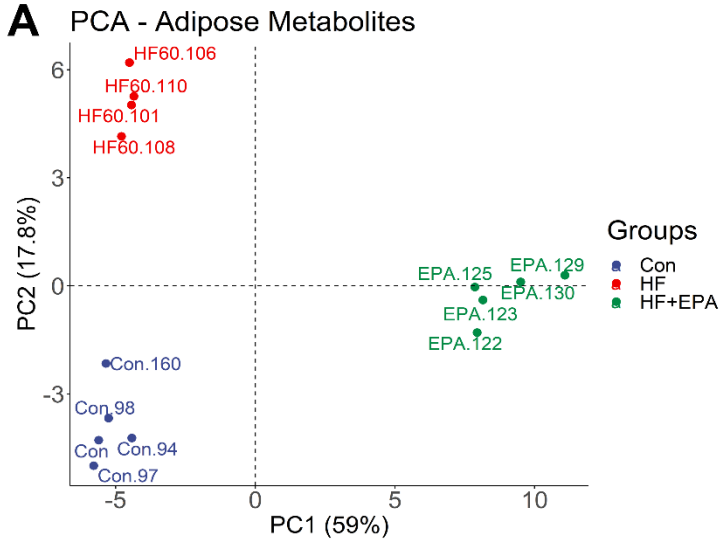

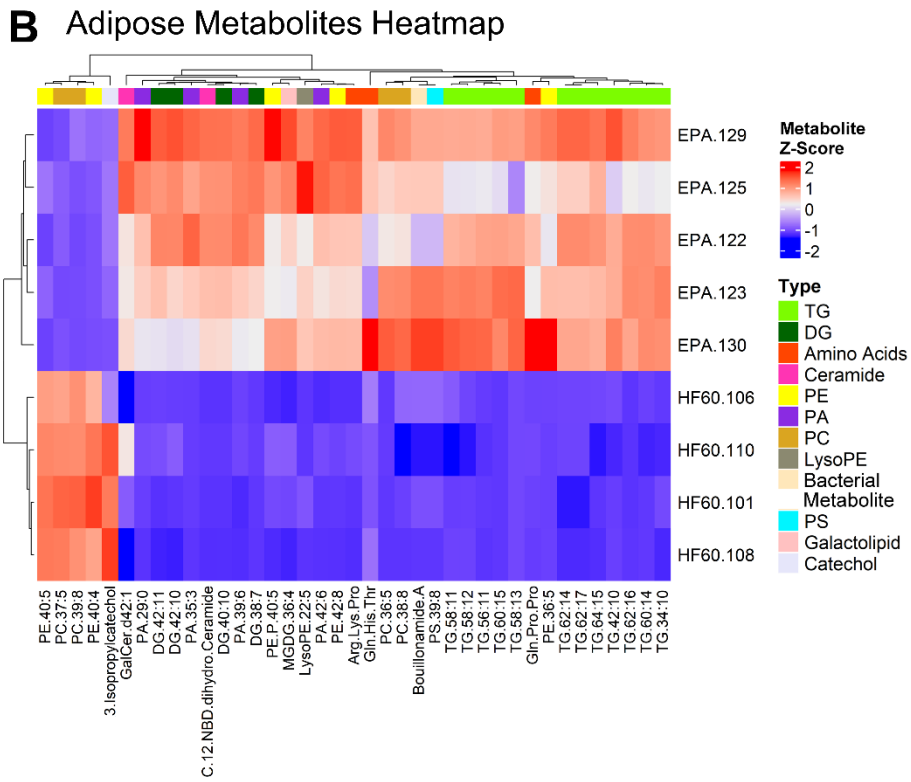

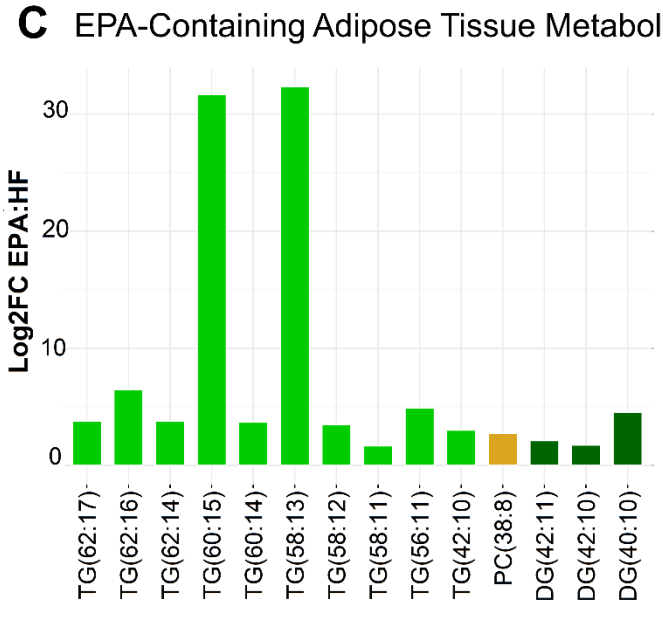

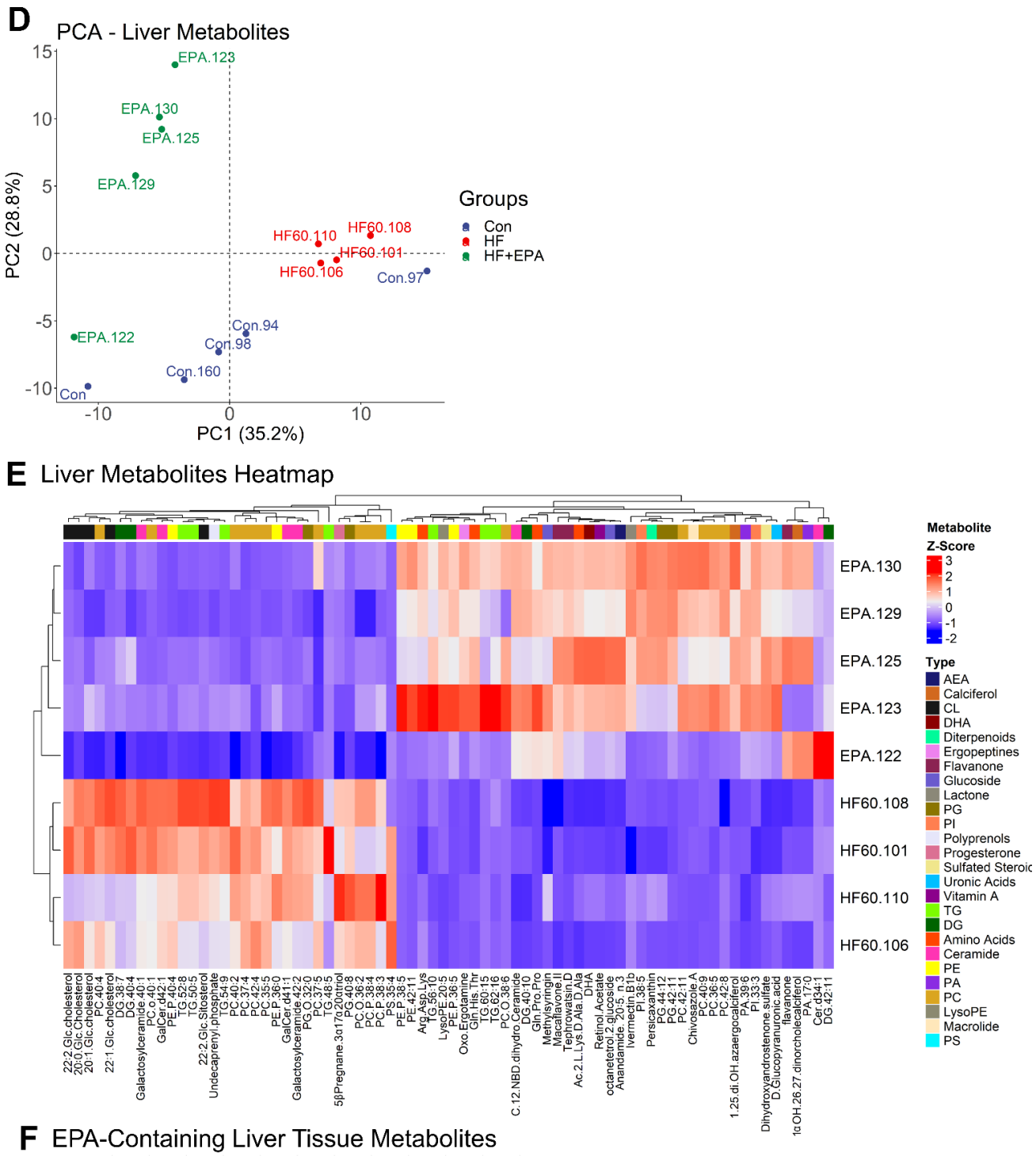

Figure 4.

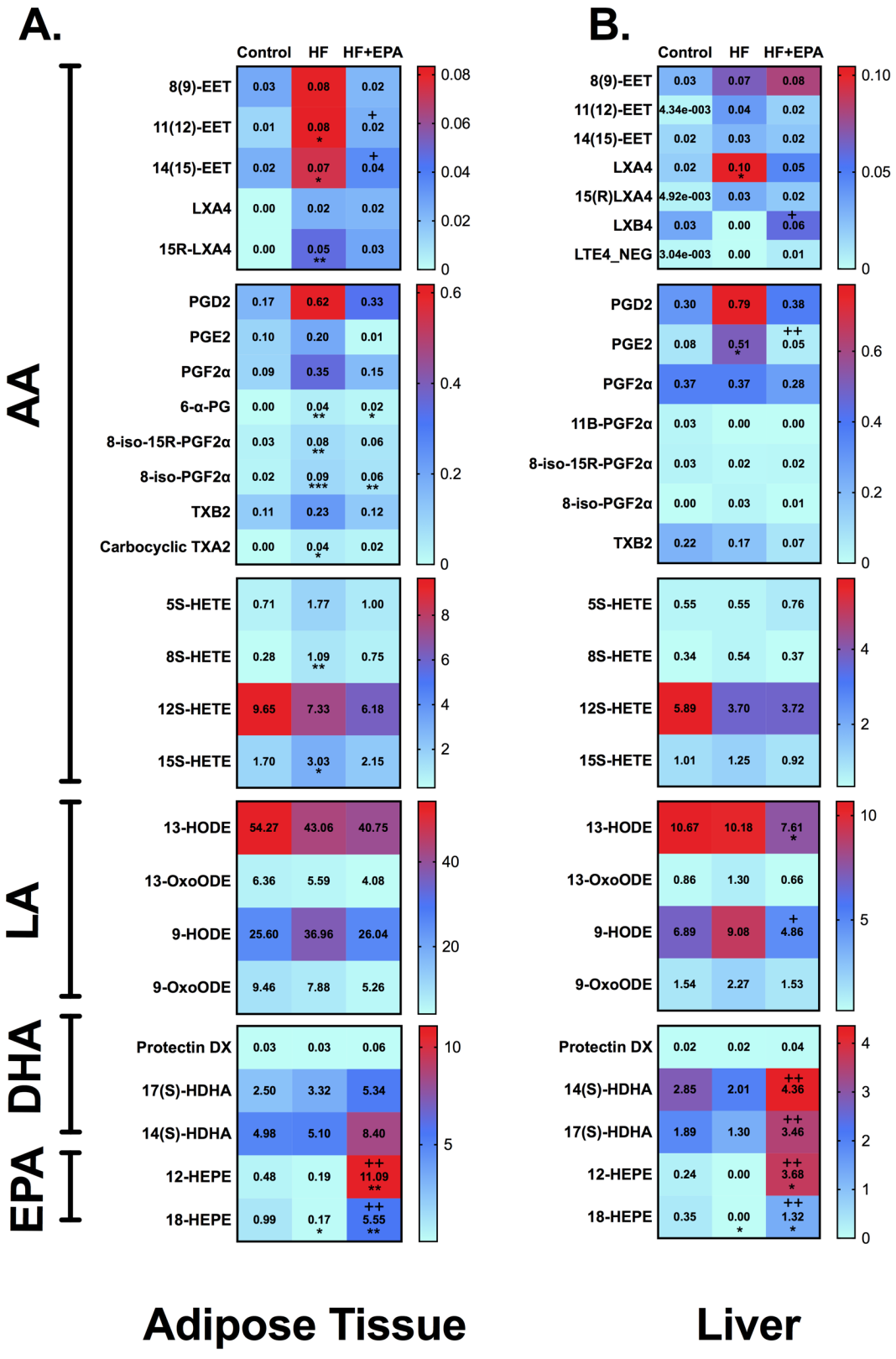

Figure 5.

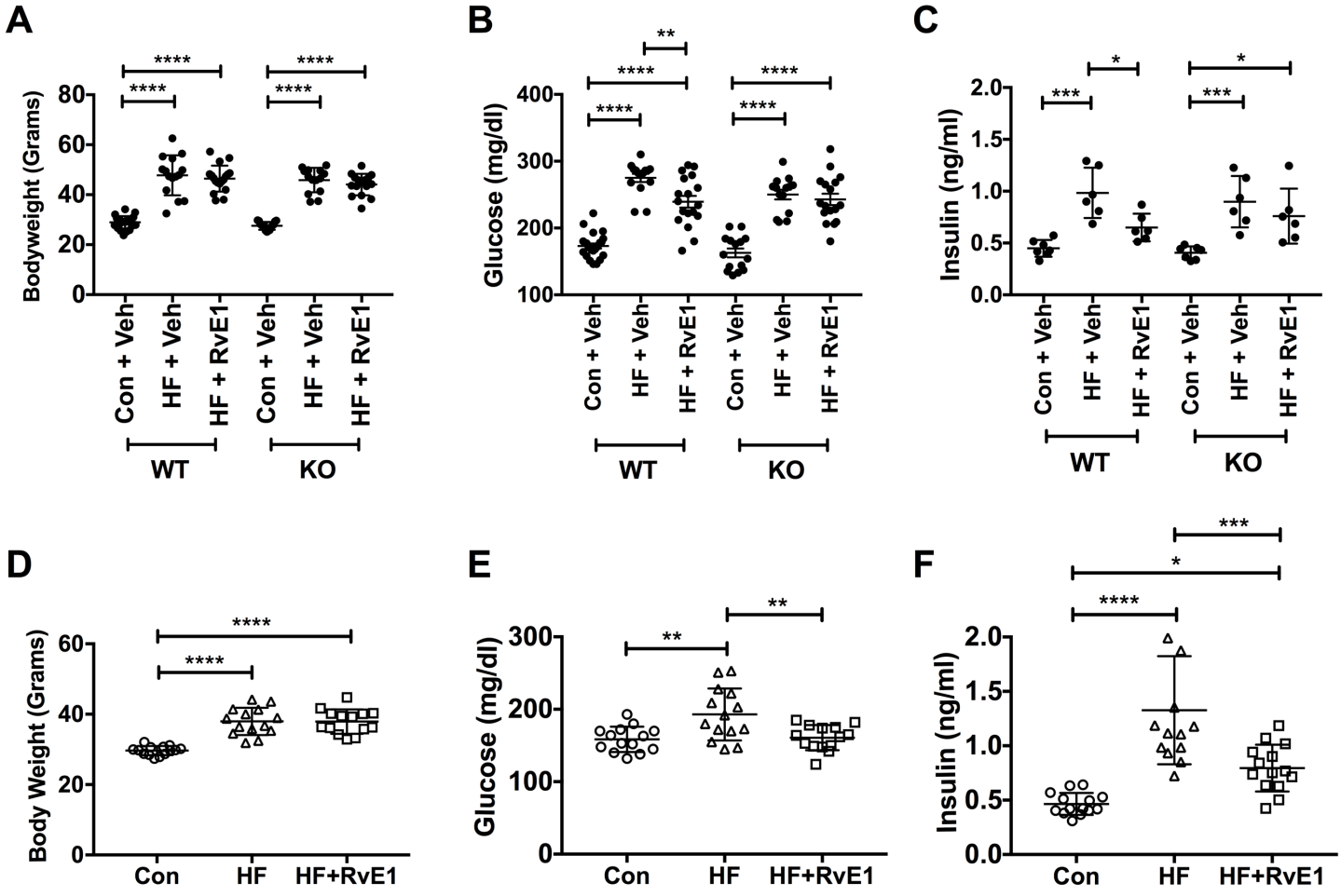

Figure 6.

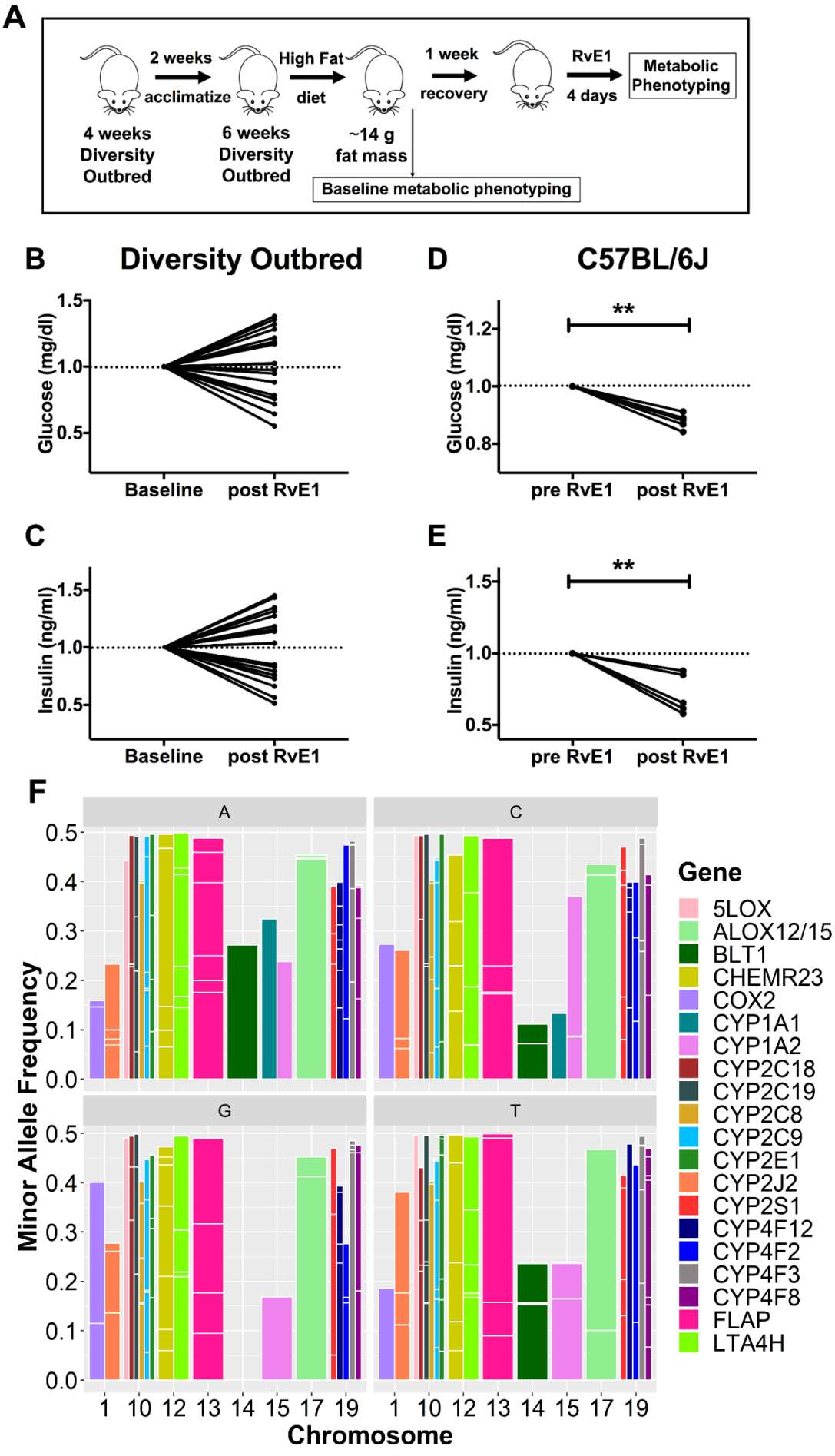

Figure 7.